

Effect of Inlet Fogging on Turbine Blade Creep Life

Agbadede, R*¹ and Allison, I²

¹Department of Electrical Engineering, Nigeria Maritime University, Okerenkoko Warri, Delta State, Nigeria.

² Nigeria Army Engineers, Lagos, Nigeria.

*Corresponding author's email: roupa.agbadede@nmu.edu.ng

Abstract

This study investigates the impact of inlet fogging on turbine blade creep life in an aero-derivative gas turbine engine. To achieve the aim of the study, an aero-derivative gas turbine engine was modelled using a gas turbine performance software, GasTurb. The modelled engine was derived from the GE LM2500 class of gas turbines. Consequent upon completing the engine modelling, ambient temperature profile data obtained from a location in Niger Delta region of Nigeria were implanted into the engine model to simulate its effect on the engine performance. Inlet fogging was simulated on the industrial gas turbine by implanting a water-to-air ratio of 0.3% (quantity of fluid injection flow rate), to cool and reduce the air inlet temperature. The outcome the investigation shows that thermal efficiency reduced with increased ambient temperature, while fuel flow and Nox severity index increased with ambient temperature. However, when inlet fogging was applied under increased ambient temperature, improvement in thermal efficiency was recorded. Also, Nox Severity index and fuel flow reduced when inlet fogging was applied under increased ambient temperature condition.

Keywords: Ambient temperature, Performance analysis, Nox severity index, Simulations, Creep life

Received: 30th January, 2021

Accepted: 2nd April, 2021

1. Introduction

High ambient/ gas turbine inlet temperatures affect the overall performance of the gas turbine, especially power output and thermal efficiency. To maintain the required/constant power output without any form of air cooling during high ambient temperatures for engines operated under constant/ base load condition, the engine is forced to operate at higher turbine inlet temperatures, thereby affecting the creep life of the turbine.

The study of Gajjar et al. (2003) described the design, installation, commissioning and operation of large-scale inlet fogging system for a combined cycle power plant. In addition, technical details and practical issues relating to inlet fogging system installation were also provided. Wang and Braquet (2008) stated that inlet fogging systems are simple and less expensive to install when compared to other power augmentation options. Also, the issue of pressure drop associated other systems is almost negligible with inlet fogging systems. In locations where fresh water is readily available, applying inlet fogging will definitely offer the best and quickest return on investment. The effect of overspray on the compressor operation was carried

out using a model derived from Tonando engine. The authors stated that wet compression caused a significant stage re-matching, moving the speed lines toward higher mass flow rate. In addition, it was stated that over spraying resulted in increased gain in efficiency and power output due to reduced compressor specific work and increased mass flow rate. A study relating to inlet fogging considerations in gas turbine ship drive application was presented in Domachowski (2015). Roumeliotis and Mathiodakis (2010) used wet compression to analyze the effects of overspray on the compressor operation and performance. Similarly, Dawoud et al. (2005) conducted an evaluation of the impact of different cooling technologies on power boosting in gas turbines. The cooling techniques were compared based on the electric energy generation enhancement. It was reported that when fog cooling technique was applied on the gas turbine, the electrical energy generated was more compared to evaporative method. Utamura et al. (1990) presented a cost estimate method to compare inlet cooling systems for power enhancement combustion turbine. System design parameters were arranged in a

dimensionless form using a conversion index. Meher-homji and Mee (2000) presented practical issues relating to high pressure inlet fogging system implementation. The study reported the use of high-pressure inlet systems which comprised specialized nozzles to create fine droplet at the inlet duct of gas turbine.

From literature search conducted, it is obvious that most studies on gas turbine inlet air cooling have either been on the comparison of the different cooling methods or the economic benefits. Even the few studies available in the open domain that relate to this work, are on the effects of relative humidity on the turbine blades creep life. This study investigates the impact of inlet fogging application of the creep life of the gas turbine.

2. Materials and methods

GasTurb performance simulation software was employed to model and simulate the application of inlet fogging on the aero-derivative gas turbine performance arising from inlet fogging. To achieve the objective of this work, design specification data for GE LM2500 obtained from open domain were used to model the twin shaft aero-derivative engine employed for the inlet fogging and turbine blade creep life investigations. Figure 1 shows the twin shaft aero-derivative engine configuration model selected from the software interface, while Table 1 presents the design point performance specifications.

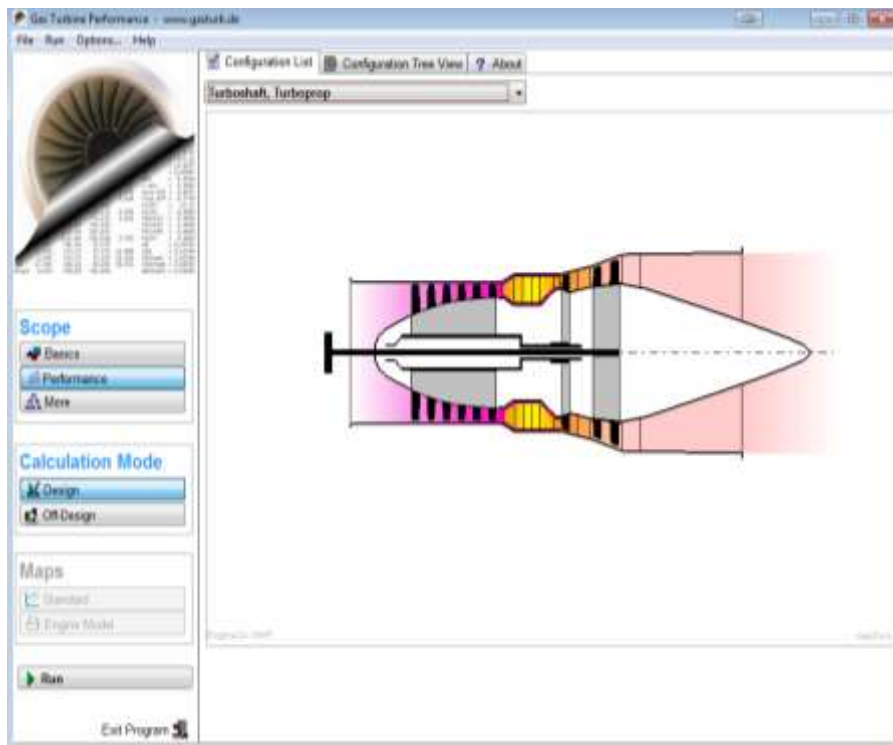


Fig. 1: Industrial gas turbine engine configuration

Table 1: Engine design specifications

Design parameters	Units
Power output	25MW
Thermal efficiency	36
PR	18
Exhaust temperature	839K
Exhaust flow	70.5kg/s
Heat rate	9705kJ/kWh

The effect of ambient temperature on the overall engine performance was simulated considering ambient temperature profile of a location in Niger Delta region, Nigeria. Based on the ambient

temperature variation profile obtained, the simulations were done by increasing the temperature from 15 to 25 degrees Celsius. Also, GasTurb software was employed to simulate the inlet fogging for the engine under investigation. Inlet fogging simulations were conducted under the increased ambient temperature conditions to improve the performance of the gas turbine. Water-to-air ratio of 0.3% recommended for inlet fogging application in (Meher-Homji and Mee, 2000; Syverud, 2007) was used to simulate the inlet fogging investigations. Table 2 shows the

Effect of Inlet Fogging on Turbine Blade Creep Life

implanted water-to-air of 0.3% of the GasTurb out using the default natural gas fuel provided in software interface, to simulate inlet fogging. All the software. gas turbine performance simulations were carried

Table 2: Inlet fogging simulation interface

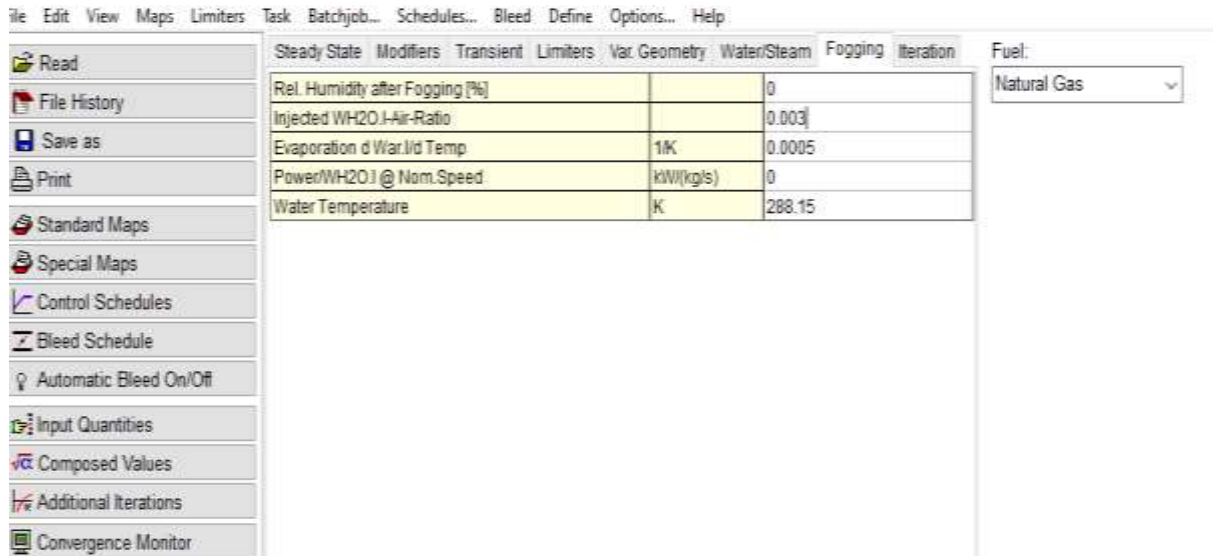


Table 3: Screen shot of blade sizing code

BLADE GEOMETRY OF LM2500 HIGH PRESSURE TURBINE BLADE USING RESULTS FROM PYTHIA SIMULATION										
Overall Specification			HP turbine - Free vortex design				At blade Mid height			
PR compres	18		ROOT	BMH	TIP	Static temperature	1415.5	1330.3		
Compo pres loss	0.96		D (NGV exit)	0.9055	0.9525235	0.9995				
TET	1527		D (Rotor exit)	0.9055	0.9525235	0.9995	Absolute mach number	0.79	0.34	
W [kg/s]	64.34	1.4752	Va		225.7469472		Axial mach number	0.32	0.33	
Power [W]	27755000		Vw3mean		115.9903219					
RPM	8000		Vwomean		514.9824326					
Cp	1418.08304	Calc.	Vwo	541.7	514.9824326	490.778	Hub to casing	ROOT	BMH	TIP
y	1.25373911	Spreadsheet calc	oo	67.377	66.32934735	66.2986	oo	67.4	66.3	65.3
Inlet Annulus Geometry			Vw3	122.01	115.9903219	110.539	oo+ain (ain=0)	67.4	66.3	65.3
P	1750896		a3	28.39	27.19440814	26.089	a1+a2	101.5	93.5	84.6
Ma	0.3	Assumption	U	379.31	398.9921107	418.67	Vo/Vin	2.60	2.49	2.39
Q	0.019249	CompFlow M=0.3	Vo	586.85	562.288707	540.208	V2/V1	1.98	2.22	2.43
A	0.07459884		Nozzle Acceleration	2.5996	2.490792075	2.39298	a3	28.4	27.2	26.1
Dmean	0.9525235	Geometric characteristic	V1	278.08	253.801968	236.984	Reaction	0.45	0.50	0.55
h	0.0468785		a1	35.728	27.19440814	17.7147				
Dtip	0.9995		V2	549.81	562.288707	575.346	Stage Overall Data			
Dhub	0.905547		a2	65.758	66.32934735	66.8981	Inlet hub/tip ratio	0.91		
HIT ratio	0.906	Assumption	Rotor Acceleration	1.9771	2.21546236	2.42779	Outlet hub/tip ratio	0.91		
Efficiency Prediction - Mean Height			V3	256.61	253.801968	251.357				
Δtstage	173.98		U	379.31	398.9921107	418.67				
Umean	398.992111									
ΔH/U ²	1.54978829	<2.5								
Valsqrt(T)	5.777	CompFlow M=0.3	TET	1527						
Va	225.746947	Stays constant								
VaU	0.56579301		x	0.47444444						
ηisent	0.9	Smith's chart-2%	cp air	1214.675631		tar	0.023466232			
Outlet Annulus Geometry			cp st01	1783.361362						
Va	225.746947		cp act	1418.083044						
T3	1353.02	Turbin exit temp	y	1.253739106						
D	0.98	Assumption	dh/dt	0.906						
D/w	630.972755		DH1	0.9995						
Vw3	115.990322									
a3	27.1944081									
V3	253.801968									
V3/sqrt(T3)	6.89990128									
M3	0.3446	CompFlow	v2/v1	1.977127649						
Q3	0.0217509	CompFlow								
R	0.51232138	1.9519 PR, Inverse PR								
P3	897921.453									
A3	0.12129785									
Aann	0.13637231									
h	0.0468785									
Dtip	0.9995									
Dhub	0.905547									
HIT ratio	0.906									
Dmean	0.9525235	Geometric characteristic								
			No of BLADES	80	Inter HPT blade spacing of 0.038					

Table 4: Screen shot of blade stress code

STRESS MODEL			
Dimensions From Scaling			
Length of Half a Section			0.005872
Centre Line to Blade RDS			0.452774
Results From Aerodynamic Analysis			
Dtip	0.9995	m	
Dhub	0.905547	m	
h	0.046977	m	
Height per section	0.011744	m	
Blade Speed	8000	RPM	
Radii from CL to the CoG of Sections From Top to Bottom			
Radius to CoG Top Sec, R1	0.493878	m	TDS-75%
Radius to CoG Second Sec, R2	0.482134	m	75%-50%
Radius to CoG Third Sec, R3	0.47039	m	50%-25%
Radius to CoG Fourth Sec, R4	0.458646	m	25%-RDS
Sectional Blade Stresses			
Density of Rene 80, ρ	8194.5		Kg/m3
π	3.142857		
First Section			
σ_1	33.38485		TDS-75%
Total Stress in First Section	33.38485		MPa
Second Section			
σ_2	32.59098		75%-50%
Total Stress in Second Section	65.97583		MPa
Third Section			
σ_3	31.79711		50%-25%
Total Stress in Third Section	97.77294		MPa
Fourth Section			
σ_4	31.00324		25%-RDS
Total Stress in Fourth Section	128.7762		MPa

Table 5: Screen shot of blade thermal model

THERMAL MODEL			
Results From Spreadsheet			
Burner Entry Temp	705.898		
Burner Exit Temp	1539.62		
Burner Temp Rise	833.722		
Case 2, RTDF=0.125	0.125		
Temperatures, RTDF=0.125			
Tmax	1643.835		
Tmin	1470.143		
Ttip	1470.143		
T75%	1643.835		
T50%	1585.938		
T25%	1528.041		
Troot	1470.143		
Sectional Blade Metal Temperatures			
Tav.sec1	1556.989		TDS-75%
Tav.sec2	1614.887		75%-50%
Tav.sec3	1556.989		50%-25%
Tav.sec4	1499.092		25%-RDS
Temp drop_tbc	150		
Sectional Blade Metal Temperatures, $\lambda=0.4$			
Cooling effectiveness	0.4		
Coolant temperature	705.898		Compre exit temp
First Section			
Tg75%	1406.989		Gas temp
Tb75%	1126.553		Blade temp
Second Section			
Tg50%	1464.887		Gas temp
Tb50%	1161.291		Blade temp
Third Section			
Tg25%	1406.989		Gas temp
Tb25%	1126.553		Blade temp
Fourth Section			
TgRDS	1349.092		Gas temp
TbRDS	1091.814		Blade temp

Table 6: Screen shot of blade creep model

Results From Thermal Model ($\epsilon=0.4$)			
	°K	°R	
Tb1	1126.553	2027.795	
Tb2	1161.291	2090.324	
Tb3	1126.553	2027.795	
Tb4	1091.814	1965.265	

Creep Life Calculations			
C	20		
First Section			TDS-75%
t_r	397401.6		hours
Second Section			75%-50%
t_r	50618.19		hours
		Life in Years	Life with FoS in Years
		5.77438	1.8492
Third Section			50%-25%
t_r	210410.6		hours
Fourth Section			25%-RDS
t_r	913845.7		hours

Results From Larson Miller Master Curve			
σ_1	33.38516	LMP	51.91
σ_2	65.97639	LMP	51.64
σ_3	97.77369	LMP	51.35
σ_4	128.7771	LMP	51.02

To estimate the creep life of the gas turbine under different operating conditions, four different codes, namely blade sizing, stress, thermal and creep models were created in separate Microsoft Excel sheets. Tables 3, 4, 5 and 6 show the screen shot of the blade sizing, stress, thermal and creep models respectively.

The following sections present description of the procedures, assumptions and equations employed to create the different models for estimating the turbine creep life. To carry out the turbine blade creep life estimation, it was only the High-Pressure Turbine (HPT) blade which was considered. This is because it is the HPT section which faces the most hazardous temperatures exiting the combustor. In order to estimate creep life of the HPT under different operating conditions, the HPT blades were first designed. The initial design data were selected based on data from Jane’s aero engines (Gunston, 1996) to scale the HPT blade coupled with a GE publication on the gas turbine. Consequently, the gas path inlet and outlet parameters at design point were obtained using GasTurB simulation software. Constant nozzle inlet angle design approach was adopted. This method was used in order to satisfy the radial

equilibrium condition, which will in addition take care of the constant mass flow per unit area requirement of all the blade radii (Ramsden, 2009).

Adopting the blade design process outlined by Ramsden (2009), the inlet and outlet geometry were sized, followed by predicting the stage efficiency using Smith’s correlation and calculating the rotor inlet velocity. Table 7 shows the blade design dimensions at the root, mean and tip obtained.

Table 7: Blade design specification

Inlet annulus geometry	
Mean diameter (m)	0.9525
Height(m)	0.0469
Tip diameter(m)	0.995
Hub diameter(m)	0.9056

In designing the blade, the following values were adopted for the blade aerodynamic parameters:

- The inlet Mach number of the HP turbine is constant at 0.3
- The axial velocity is constant at 226m/s
- The HP turbine speed of 8000RPM obtained from the performance simulations was adopted.
- Cooling effectiveness of 0.4 was adopted.

Equation (1) was used to calculate the cooling effectiveness (ϵ), and it also shows how the gas stream temperature T_g , blade metal temperature (T_b) and the coolant temperature are related to the cooling effectiveness.

$$\epsilon = \frac{T_g - T_b}{T_g - T_{c1}} \quad (1)$$

The multi-dimensional stresses and strains arising from load-imposed conditions and the non-uniform temperature distribution exiting from the combustor have made the prediction of the turbine blade creep life difficult. Assuming a uniform stress and temperature could prevent these problems when estimating the creep life of turbine blades. In order to achieve a more accurate result, radial temperature distribution factor (RTDF) is employed to estimate the blade creep life in this study. Turbine blades, due to their rotation, experience average circumferential temperatures in a given radial plane. The RTDF which affects the rotor blade life when employing measured circumferential values is used to calculate the temperature variation at each section of the blade. According to Walsh and Fletcher (2004), the controlled value of RTDF should be less than 20%. Equation (2) gives the RTDF calculation:

$$RTDF = T_{max} - TET / (TET - T_3) \quad (2)$$

where T_{max} is the Circumferentially mean outlet peak temperature, TET is the Mean temperature, and $TET - T_3$ is the Mean Combustor temperature rise. Also, based on the assumption that the maximum temperature will occur at the 75% blade height, the following formulae were derived. Calculations of maximum and minimum temperatures are thus given below (Eshati et al., 2010):

$$T_{max} = T_{RI} + (\Delta T_{burner} X RTDF) \quad (3)$$

$$T_{min} = (5T_{RI} - 2T_{max}) / 3 \quad (4)$$

T_{RI} is the Rotor inlet relative gas temperature (K), and ΔT_{burner} is the Temperature rise at burner (K)

The assumptions which were made in this study are (Eshati et al., 2010):

- The minimum gas temperature occurs at the root and tip of the blade
- Linear rise of gas temperature from root to 75% of the blade span
- Linear reduction in gas temperature from maximum to the blade tip
- The average of the root datum section temperature (T_{RDS}), temperature at 75% of blade height ($T_{75\%}$) and top datum section temperature (T_{TDS}) equal the turbine inlet temperature

It was also assumed that the cooling air temperature will remain the same at all sections of the blade. The metal temperature, T_b , is given in Equation (5). T_b as a function of the cooling effectiveness, gas and coolant temperatures as highlighted in Equation (5).

$$T_b = T_g - \epsilon (T_g - T_c) \quad (5)$$

In estimating the blade section metal temperatures, each section was treated as an individual blade, where the metal temperature was assumed to be constant. In addition, the cooling effectiveness and cooling air temperatures were assumed to be same at all the blade sections. In reality, this cannot be completely correct because there would be temperature variation from the entrance of the blade to the exit (Laskaridis, 2009). However, for the purpose of this study, it is assumed that the coolant temperature is the same for all the blade sections.

According to Laskaridis (2009), the gas temperature equals the difference between the turbine inlet temperature and the temperature drop due to Thermal Barrier Coating (TBC):

$$T_g = TET - \Delta T_{tbc} \quad (6)$$

According to Blackie (2008), centrifugal stress only contributes about 70-90% of the total blade stress. Hence, it is only centrifugal force that was considered for calculating the stress model in this study. Also, in considering the stress analysis, the blade was divided into four sections: stress acting at root datum section (RDS), 25%, 50% and 75% of blade height. Centrifugal Force experienced by the blade was calculated using Equation (7).

$$Centrifugal\ force, CF = mr\omega^2 \quad (7)$$

where m is the mass of blade in kg, r is the radius at centre of gravity, ω is the rotational speed in

rads/sec. Mass of blade = density of blade x volume of blade. Substitute mass of blade into Equation (7) gives Equation (8).

$$CF = Ah\rho r \left(\frac{2\pi N}{60}\right)^2 \quad (8)$$

$$\sigma CF = \frac{CF}{A} \quad (9)$$

where CF is Centrifugal Force, A is Blade's cross-sectional area, ρ is Density of the blade material, h is Blade height, r is Radius at centre of gravity, N is Blade Rotational Speed, and σCF – Centrifugal stress.

As can be seen in Fig. 2, the blade height was divided into four equal sections and the distances from the Centre Line (CL) to the Root Datum Section (RDS) is taken into consideration to compute the height at various sections of the blade. This approach adopted is similar to the method employed by Allison (2010), to calculate the centrifugal force at different sections of the blade. Radius from CL to Centre of Gravity (CoG) of first section, at 25% blade height = 0.4586475m

Radius from CL to CoG of second section, 25 % blade height - mid blade height = 0.4703925m

Radius from CL to CoG of third section, mid blade height – 75% blade height= 0.4821375m

Radius from CL to CoG of fourth section, TDS – 75% blade height = 0.4938825m

From the material properties of René 80, the blade density, $\rho = 8194.5\text{Kg/m}^3$

Also, the rotational speed of the blade, $N = 8000\text{RPM}$

Therefore, the stresses at different blade sections were calculated using Equation (9).

The stresses at the various blade sections are computed in Table 8. The stresses calculated at the various sections of the blade were used to obtain LMP (Larson Miller Parameter) from Master curve of the blade material. Consequently, the LMP and blade metal temperature at the blade sections were used to estimate the rupture time and the blade creep life for different conditions investigated. For brevity, it is only the screen shot for the model estimating the creep life of the turbine blade operated high ambient temperature with inlet fogging application is presented in Table 9.

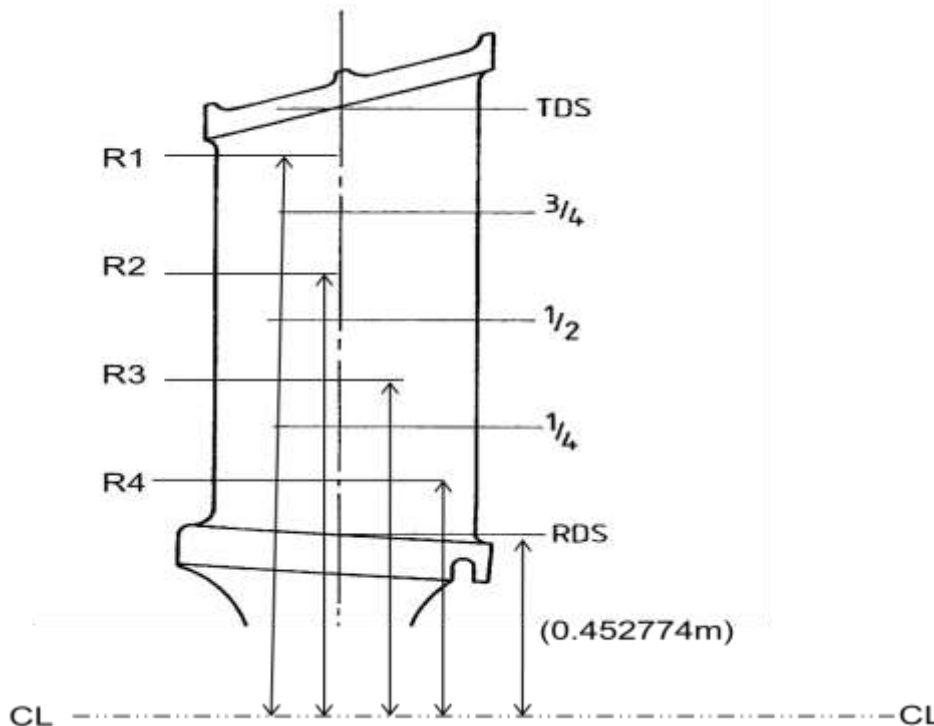


Fig. 2: Sized turbine blade indicating the different sections

Table 8: Stress at various sections of the blade

Blade section	Stress introduced	Total stress in section
Top datum section (TDS)-75% Blade span	$\sigma_{CF}=33.3\text{MPa}$	Total stress acting at TDS-75% blades span, $\sigma_{CF}=33.3\text{MPa}$
Mid blade span -75% blade span	$\sigma_{CF}=32.5\text{MPa}$	Total stress acting at 25 % blades span, $\sigma_{CF}=97.5\text{MPa}$
25% blade span –Mid blade span	$\sigma_{CF}=31.7\text{MPa}$	Total stress acting at 50 % blades span, $\sigma_{CF}=65.8\text{MPa}$
Root datum section – 25% blade span	$\sigma_{CF}=30.9\text{MPa}$	Total stress acting at RDS, $\sigma_{CF}=128.5\text{MPa}$

Table 9: Turbine blade creep life model for inlet fogging application

Results From Thermal Model ($\alpha=0.4$)			
	*K	*R	
Tb1	1126.553	2027.795	
Tb2	1161.291	2090.324	
Tb3	1126.553	2027.795	
Tb4	1091.814	1965.265	
Creep Life Calculations			
C	.20		
First Section		TDS-75%	
t_r	397401.6	hours	
Second Section		75%-50%	
t_c	50618.19	hours	
			Life in Years
			5.77438
			Life with FoS in Years
			3.8492
Third Section		50%-25%	
t_r	210410.6	hours	
Fourth Section		25%-RDS	
t_r	913845.7	hours	
Results From Larson Miller Master Curve			
σ_1	33.38516	LMP	51.91
σ_2	65.97639	LMP	51.64
σ_3	97.77369	LMP	51.35
σ_4	128.7771	LMP	51.02

3. Results and discussion

3.1 Engine performance analysis

Figures 3, 4 and 5 show the plots of thermal efficiency, fuel flow and NO_x severity index against different operating conditions. As can be seen in Figure 3, when ambient temperature was increased from design condition of 15°C to 25°C, the thermal efficiency dropped from 36.3% to 35.7%. However, when fogging was applied to the case with increased ambient temperature 25°C, the thermal efficiency increased 35.7% to 36.2%. The increased thermal efficiency with fogging system can be attributed to increased pressure ratio, thereby causing the thermal efficiency to increase. In the case of fuel flow plot presented in Fig. 4, the

plot shows that fuel flow increased from design condition of 1.413 to 1.433kg/s. The increase in fuel flow with ambient is as a result of the reduced power output; hence necessitating an increase in fuel flow to meet the required load demand under high ambient temperature. As can be seen in Fig. 5, when ambient temperature was increased from design condition of 15°C to 25°C, Nox severity index increased also increases. This is expected because at increased ambient temperature of 25°C, the compressor exit temperature is higher than the design condition. Hence, higher NO_x severity index is expected because it is associated with higher combustion temperatures.

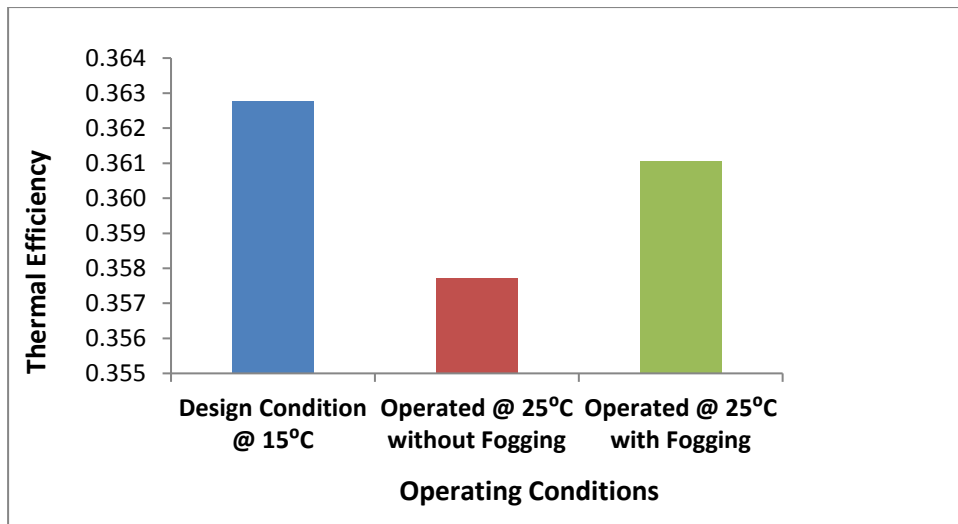


Fig. 3: Thermal efficiency against ambient temperature

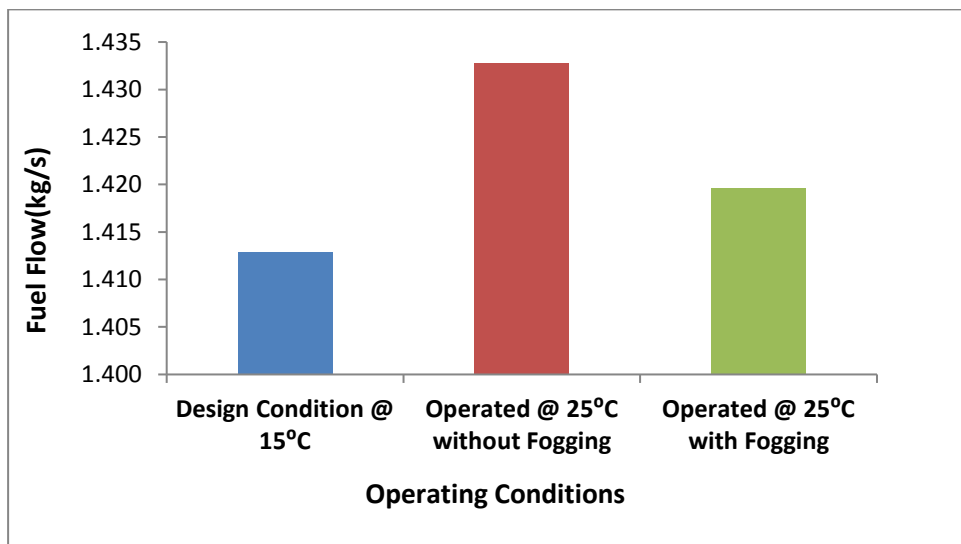


Fig. 4: Fuel Flow against ambient temperature

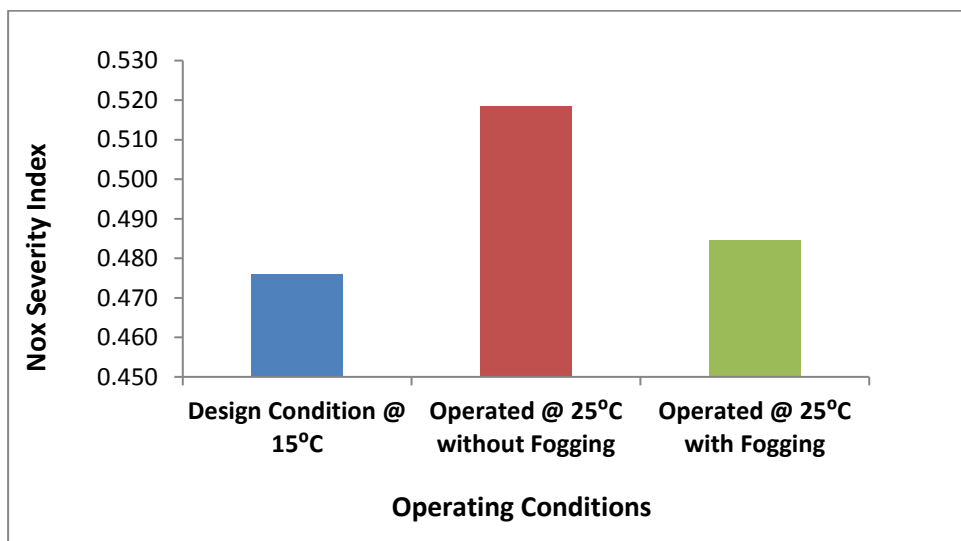


Fig. 5: NO_x Severity Index against ambient temperature

Figure 6 shows the bar chart plots of turbine's blade time to rupture for the different operating conditions. When the turbine's blade time to rupture for the case without fogging application and that of fogging were compared, plots show that the time to rupture for the case without fogging is about 16,000 hours as against 50,000 hours for the case where fogging system is employed. Converting from hours to years shows that the turbine blade time to rupture for the engine operated without fogging is about 2years, while for

the engine where fogging system is used is approximately 6years (see Fig. 7). The time to rupture obtained for the different scenarios investigated seems reasonable because Weber et al. (2005) predicted hot section repair and retirement interval for Rene' 80 direction alloy at 25,000 and 50,000hours respectively. Saravanamuttoo et al. (2009) stated that the nominal operating lives for gas turbines are in the range of 10,000 to 100,000 hours. In addition, the blade material considered in this study was the Rene' 80 materials.

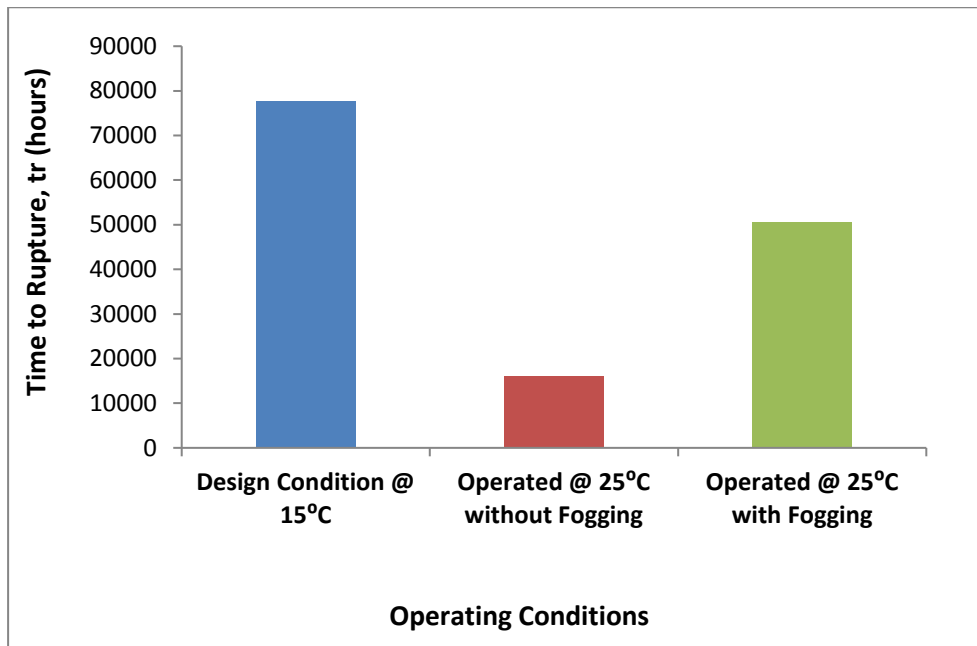


Fig. 6: Turbine blade time to rupture for engines operated under different conditions

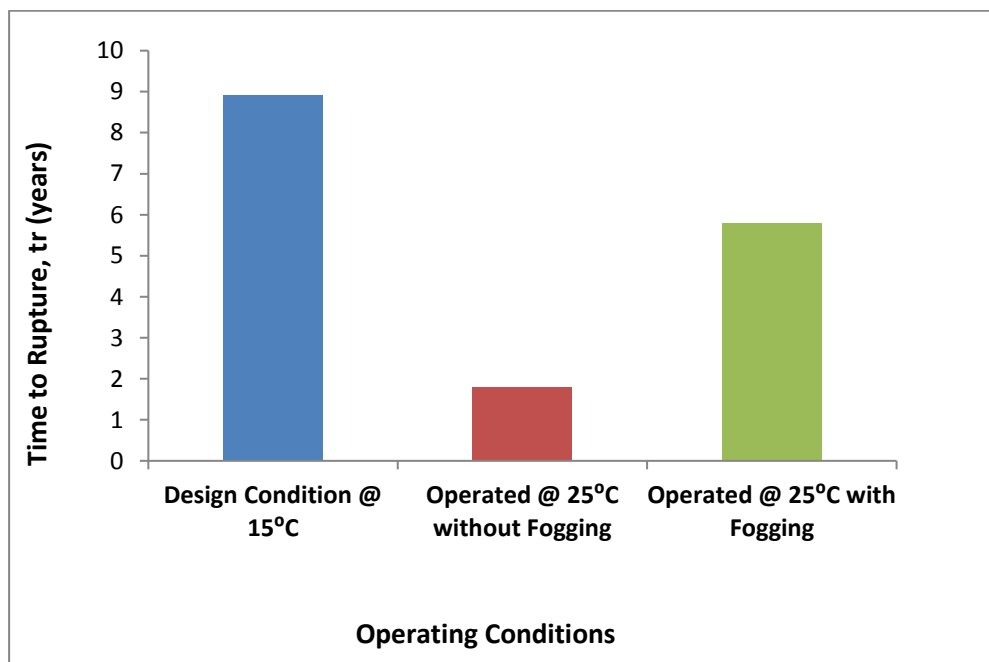


Fig. 7: Turbine blade creep life for engines operated under different conditions

4. Conclusions

This study presents effects of inlet fogging application on the turbine blade creep life. GasTurb performance simulation was employed to model and simulate the performance of the gas turbine under fogging and no fogging conditions. Inlet fogging simulations were conducted using the GasTurb simulation software where water-to-air of 0.3% was implanted into the software. The findings drawn from the study are:

- a. Thermal efficiency reduced with increased ambient temperature
- b. Fuel flow and Nox severity index increased with ambient temperature
- c. Thermal efficiency of the engine improved when inlet fogging system is implemented
- d. Engine operated with inlet fogging in use demonstrates reduced fuel flow and Nox severity index when compared with the case without inlet fogging

Acknowledgement

The authors are exceedingly grateful to Nigeria Maritime University for the technical support.

References

- Wang, T. and Braquet, L. (2008) Assessment of inlet cooling to enhance power output of a fleet of gas turbines. Proceedings of Industrial Energy Technology Conference IETC 30th, May 6-9, 2008, New Orleans, USA.
- Gajjar, H., Chaker, M., Dighe, A. and Meher-Homji, C.B. (2003) Inlet fogging for a 655mw combined cycle power plant – design, implementation and operating experience. Proceedings of ASME Turbo Expo 2003, June 16-19, 2003, Atlanta, Georgia, USA.
- Domachowski, Z. and Dzida, M. (2015) Inlet air fogging of maritime gas turbine power output compensation. Polish Maritime Research, 22: 53-58.
- Roumeliotis, I. and Mathioudakis, K. (2010) Evaluation of water injection effect on compressor and engine performance and operability. Applied Energy, 87:1207-1216.
- Dawoud, B., Zurigat, H.Y. and Bortmany, J. (2004) Thermodynamic assessment of power requirement and impact of different gas turbine inlet air cooling techniques at two different locations in Oman. Applied Thermal Engineering, 25:1579-1598.
- Utamura, M., Nishimura, Y., Ishikawa, A. and Ando, N. (1996) Economics of gas turbine inlet air cooling system for power enhancement. ASME Turbo Expo, June 10-13, 1996, Birmingham, UK.96-GT-516.
- Meher-Homji, C.B., and Mee, T. (2000) Inlet fogging of gas turbine engines – part b: practical considerations, control and o&m aspects. Proceeding of ASME Turbo Expo 2001, Paper No. 2000-GT-308, May 8-11, 2000, Munich, Germany.
- Syverud, E. (2007) Axial compressor performance deterioration and recovery through online washing. PhD Thesis, Norwegian University of Science and Technology.
- Gunston, B. (1996). Jane's Aero-Engines, Issue Eleven, Jane's Information Group, England.
- Ramsden, K.W. (2009) Gas turbine fundamentals and turbomachinery. MSc Lecture Notes, Department of Thermal Power, School of Engineering, Cranfield University, UK.
- Walsh, P.P. and Fletcher, P. (2004) Gas turbine performance. 2nd Ed, Blackwell Science, Limited, Oxford, UK
- Eshati, E., Abdul Ghafir, M.F., Laskaridis, P. and Li, Y.G. (2010) Impact of operating conditions and design parameters on gas turbine hot section creep life. Proceedings of ASME Turbo Expo 2010: Power for Land, Sea and Air, June 14-18, 2010, Glasgow, UK, ASME.
- Laskaridis, P. (2009) Gas turbine lifing. Unpublished Fatigue and Fractures Course Notes, Department of Thermal Power, School of Engineering, Cranfield University, UK.
- Blackie, J. (2008) Engine lifing analysis-an assessment of creep, diffusion and cyclic oxidation of HPT blades comprised of cmsx-4 base material and Nial coating. MSc Thesis, Cranfield University, UK.
- Weber, B., Jin, H. and Pistor, R. and Lowden, P. (2005) Application of an integrated engineering approach for Im1600 blade life on-line assessment. 16th Symposium on Industrial Application of Gas Turbines, October 12-14, 2005, Banff, Alberta, Canada.
- Saravanamutto, H.I.H., Rogers, G.F.C., Cohen, H. and Straznicky, P.V. (2009) Gas turbine theory. 6th Ed. Pearson Education Limited, Edinburgh Gate Harlow, Essex, England.